PDFgetN3: atomic pair distribution functions from neutron powder diffraction data using ad hoc corrections

Juhas, Pavol; Louwen, Jaap N.; van Eijck, Lambert; Vogt, Eelco T.C.; Billinge, Simon J.L.

DOI
10.1107/S1600576718010002

Publication date
2018

Document Version
Final published version

Published in
Journal of Applied Crystallography

JOURNAL OF APPLIED CRYSTALLOGRAPHY
ISSN 1600-5767

PDFgetN3: atomic pair distribution functions from neutron powder diffraction data using *ad hoc* corrections

Pavol Juhás,[a] Jaap N. Louwen,[b] Lambert van Eijck,[c] Eelco T. C. Vogt[b,d] and Simon J. L. Billinge[e,f]*

[a]Computational Science Initiative, Brookhaven National Laboratory, Upton, NY 11973, USA, [b]Albemarle Catalysts Company BV, PO BOX 37650, 1030 BE Amsterdam, The Netherlands, [c]Department NPM2/RST, Faculty of Applied Sciences, Delft University of Technology, Delft, The Netherlands, [d]Debye Institute of Nanomaterials Science, Utrecht University, Universiteitsweg 99, 3584 CG Utrecht, The Netherlands, [e]Department of Applied Physics and Applied Mathematics, Columbia University, New York, NY 10027, USA, and [f]Condensed Matter Physics and Materials Science Department, Brookhaven National Laboratory, Upton, NY 11973, USA. *Correspondence e-mail: sb2896@columbia.edu

Received 7 May 2018
Accepted 11 July 2018

Edited by Th. Proffen, Oak Ridge National Laboratory, USA

Keywords: neutron diffraction; pair distribution functions; constant-wavelength neutron instruments; computer programs.

PDFgetN3, a new software tool for the extraction of pair distribution functions (PDFs) from neutron powder diffraction intensity data, is described. Its use is demonstrated with constant-wavelength neutron data measured at the new powder diffractometer PEARL at the Delft University of Technology. *PDFgetN3* uses an *ad hoc* data collection protocol similar to *PDFgetX3*. The quality of the resulting PDFs is assessed by structure refinement and by comparison with established results from synchrotron X-ray scattering.

1. Introduction

The analysis of total scattering and pair distribution functions (PDFs) has become increasingly popular in the field of nanomaterial structural analysis (Egami & Billinge, 2012). Nanomaterials often do not display sufficient long-range order to allow traditional structure analysis by diffraction measurements (Billinge, 2010). A number of beamlines for both X-rays and neutrons have been optimized for total scattering and PDF analysis (Egami & Billinge, 2012). Raw data from these instruments need to be processed by correcting for experimental artifacts and normalizing. Several software tools are available to extract the PDF from the scattering patterns, such as *GudrunX* (Soper & Barney, 2011; http://www.isis.stfc.ac.uk/instruments/sandals/data-analysis/gudrun8864.html), *RAD* (Petkov, 1989) and *PDFgetX2* (Qiu *et al.*, 2004) for X-rays, and *GudrunN* (http://www.isis.stfc.ac.uk/instruments/sandals/data-analysis/gudrun8864.html) and *PDFgetN* (Peterson *et al.*, 2000) for neutrons. These programs all use elaborate correction algorithms that require a multitude of complicated user inputs. The program *PDFgetX3* (Juhás *et al.*, 2013), which uses an *ad hoc* correction algorithm, was developed to overcome this problem. It was found to produce PDFs of comparable quality to those obtained using *PDFgetX2*, which implements all the corrections, but with much less user input and much more quickly.

All the tools described above are for X-ray or time-of-flight neutron analysis. There are few options for obtaining the PDF from constant-wavelength neutron data. The existing codes are available as instrument-specific utilities (Fischer, 2016; Howe & McGreevy, 1996), which are not easy to obtain and use elsewhere. The new software *PDFgetN3* introduced here

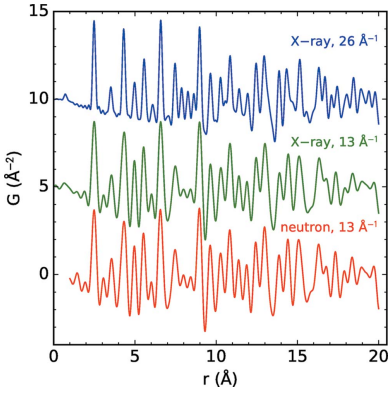

provides the PDF extraction capability in a freely available, user-friendly, software program. While developed for constant-wavelength intensity *versus* 2θ data, the program has also been successfully tested with intensity *versus* Q data acquired from a time-of-flight instrument.

The PDF in the $G(r)$ form is calculated by Fourier transformation of the reduced structure function (also called 'interference function') $F(Q)$ (Egami & Billinge, 2012):

$$G(r) = (2/\pi) \int_{Q_{\min}}^{Q_{\max}} F(Q) \sin Qr \, \mathrm{d}Q, \quad (1)$$

where $F(Q)$ is expressed in terms of the structure function, $S(Q)$, as

$$F(Q) = Q[S(Q) - 1], \quad (2)$$

and $S(Q)$ derives from the coherent scattering intensity normalized per atom $I_c(Q)$. For the case of X-ray scattering, $S(Q)$ is given by

$$S(Q) = \frac{I_c(Q) - \langle f_i(Q)^2 \rangle + \langle f_i(Q) \rangle^2}{\langle f_i(Q) \rangle^2}, \quad (3)$$

where $f_i(Q)$ is the Q-dependent X-ray scattering factor of atom i, and the averaging is done over all atoms. In general, the coherent intensity I_c is extracted from the measured intensity I_m by correcting for a number of contributions to the intensity that multiply or add to the coherent signal:

$$I_m(Q) = \alpha(Q) I_c(Q) + \beta(Q). \quad (4)$$

Incoherent Compton and background scattering contribute to the additive corrections, whereas self-absorption and polarization contribute to the multiplicative corrections.

Billinge & Farrow (2013) showed that it is possible to get a sufficiently accurate estimate of $\alpha(Q)$ and $\beta(Q)$ for X-ray scattering by applying an *ad hoc* approach. Although the method was developed for X-ray scattering it also works for neutron scattering, by applying a small change to the structure function $S(Q)$:

$$S(Q) = \frac{I_c(Q) - \langle b_i^2 \rangle + \langle b_i \rangle^2}{\langle b_i \rangle^2}, \quad (5)$$

where b_i is the (Q-independent) coherent neutron scattering length of atom i, and the angle brackets indicate an average over all atoms in the sample. Finally, the adjusted $S(Q)$ feeds into equations (2) and (1) to allow calculation of the PDF.

1.1. PEARL diffractometer

The neutron powder diffractometer PEARL at TU Delft is a constant-wavelength (CW) diffractometer. The wavelength of the neutrons that impinge on the sample in such CW instruments is selected from a polychromatic neutron beam by a monochromator. Upstream of the monochromator and downstream towards the sample, Soller collimators are placed in the neutron beam, as well as between the sample and the neutron detector. Together with the so-called take-off angle of the neutrons reflected from the monochromator, the three collimators define the instrumental resolution of a CW diffractometer (Caglioti *et al.*, 1958). PEARL is based at the 2 MW research reactor of TU Delft (van Eijck *et al.*, 2016). Despite the relatively low brilliance of this neutron source, the diffractometer can be considered a rather competitive medium-resolution instrument owing to its high take-off angle at the monochromator and the lack of collimators. The measuring time for typical samples ranges from 10 min to a day depending on the sample (crystal symmetry, neutron scattering cross section, amount of sample *etc.*). The instrument was conceived to operate at standard wavelengths of 2.51, 1.67 and 1.33 Å, but because of its placement on a radial beam tube that looks directly towards the reactor core, shorter-wavelength under-moderated neutrons are available at a reasonable flux loss compared with the standard settings. The shorter wavelengths allow us to collect the diffraction pattern up to $Q = 13$ Å^{-1}. As such, besides the typical powder diffraction used to study crystals that exhibit long-range order, PEARL can be used to perform PDF analysis of samples that lack such long-range order. Short-range order can be found in amorphous systems, in nanostructures, and, for instance, in the catalytically active sites of metal–organic frameworks (MOFs) and zeolites. To extract such short-range order from a high-Q diffraction pattern, a PDF analysis is required.

1.2. The *PDFgetN3* program

PDFgetN3 is released bundled in a Python package `diffpy.pdfgetx`, which can be obtained from http://www.diffpy.org. An updated version of the *PDFgetX3* tool for X-rays (Juhás *et al.*, 2013) is also included. The data conversion in *PDFgetN3* acts as a chain of simple transformations that take a pair of input vectors (x_{in}, y_{in}) and return transformed values (x_{out}, y_{out}). The transformations can be listed from the *PDFgetN3* interactive prompt using the `pdfgetter.describe()` function and their respective intermediate outputs are available in the `pdfgetter.results` variable. The chain of transformations is configurable and can be extended with user-defined operations. The *PDFgetN3* and *PDFgetX3* programs have two pre-defined configuration modes, 'neutron' and 'xray', which set up transformations suitable for processing neutron or X-ray powder data. The essential difference between the modes is in using constant neutron scattering lengths *versus* Q-dependent X-ray scattering factors for the intensity normalization in equation (5). The configuration modes can be selected by passing the `--mode` option to the program and thus running the `pdfgetn3` program is equivalent to executing `pdfgetx3 --mode=neutron`. Besides the neutron mode, the new release of *PDFgetN3*/*PDFgetX3* provides an additional parameter, `twothetazero`, to correct for goniometer offset in the scattering data. The parameter specifies the actual zero angle in diffractometer degrees and has proved crucial for obtaining high-quality PDFs from the PEARL data. Another major development in the new software is the added support for Python 3 (versions 3.4 or later) with a compatibility to Python 2.7 preserved. The software release also includes numerous bug fixes to

PDFgetX3 and required updates for the developments of third-party libraries.

Because neutron scattering lengths are independent of Q, *PDFgetN3* displays some specific behaviors that are different from the X-ray case. First, the obtained PDF is independent of the chemical composition used in data processing. Different chemical formulas result in a constant PDF re-scaling proportional to $\langle b_i^2\rangle/\langle b_i\rangle^2$, but otherwise the shape of the obtained curves is identical. *PDFgetN3* also shows a similar re-scaling behavior after subtraction of a constant background B from the input raw intensities. The overall PDF scale changes as

$$C(B) = \frac{\langle I_\mathrm{m}\rangle - B}{\left[\langle I_\mathrm{m}\rangle - B\right]^2 + \left[\mathrm{std}(I_\mathrm{m})\right]^2}, \qquad (6)$$

where $\mathrm{std}(I_\mathrm{m})$ is the standard deviation of all raw intensities and $\langle I_\mathrm{m}\rangle$ their average. The maximum PDF scale is then attained at

$$B = B_\mathrm{max} = \langle I_\mathrm{m}\rangle - \mathrm{std}(I_\mathrm{m}). \qquad (7)$$

This is because background-corrected intensities are rescaled to the order of $\langle b_i\rangle^2$ before passing to equation (5), which changes the output signal scale, while the constant offset is completely filtered away by the polynomial correction for the structure-independent signal (Juhás *et al.*, 2013).

2. Experimental

The procedure was tested with samples of nickel and a NIST standard sapphire (α-Al_2O_3, corundum) recorded at the PEARL diffractometer at room temperature using the 755 reflection in the germanium monochromator, resulting in a constant neutron wavelength of 1.098 Å. Data were collected over a 2θ range of 10.58–158.98° with a pixel angular width of approximately 0.105°. This corresponds to Q values ranging from 1.056 to 11.253 $Å^{-1}$. The data were collected in 21 h for sapphire and 80 min for nickel. Instrumental background and scattering intensities from the vanadium sample holder were measured separately.

X-ray measurements for comparison were carried out at the XPD (28-ID-2) powder diffractometer at the National Synchrotron Light Source II (NSLS-II), Brookhaven National Laboratory. The sapphire powder was placed in a 0.7 mm-thick glass capillary and mounted perpendicular to the monochromatic X-ray beam of 0.2370 Å wavelength. The scattering intensities were collected at room temperature using a PerkinElmer flat-panel aSi detector positioned 207 mm behind the sample. The exact detector distance and orientation were calibrated using the *FIT2D* (Hammersley *et al.*, 1996; Hammersley, 2016) program, which was also utilized to integrate pixel counts into a one-dimensional intensity *versus* Q powder pattern. Finally, the data were corrected for empty capillary background and transformed to PDFs with the *PDFgetX3* software (Juhás *et al.*, 2013).

The neutron diffraction patterns were analyzed by the Rietveld method using the *GSAS-II* program (Toby & Von Dreele, 2013). The neutron PDFs (and the comparison X-ray PDFs) were further analyzed by PDF structure refinements using the *SrFit* package embedded in the *DiffPy-CMI* software (Juhás *et al.*, 2015). This allowed for automated iterative refinement of the relevant structure parameters as well as the zero offset of the diffractometer angle and the neutron wavelength (at a fixed unit cell).

Table 1
Rietveld (*GSAS-II*) analysis results for the PEARL neutron powder diffraction data recorded at a wavelength of 1.098 Å.

	Nickel	Sapphire
a (Å)	3.5244	4.7594†
c (Å)	–	12.9923†
U_iso ($Å^2$)	0.00476	0.00279 (Al), 0.00327 (O)
Zero correction (°)	−0.1742	−0.158
R_w	0.046	0.075

† Fixed value from NIST certificate.

3. Results

3.1. Rietveld refinement of the diffraction patterns

The empty can and vanadium sample holder background were removed prior to Rietveld analysis. An additional background was fitted using a simple three- or five-parameter Chebyshev polynomial. Instrumental line broadening profiles were determined using a sapphire NIST standard. The diffraction patterns for nickel and sapphire are displayed in Fig. 1 together with the respective Rietveld refinements.

The refined parameters can be found in Table 1. The refined cell constants for nickel are in good agreement with values

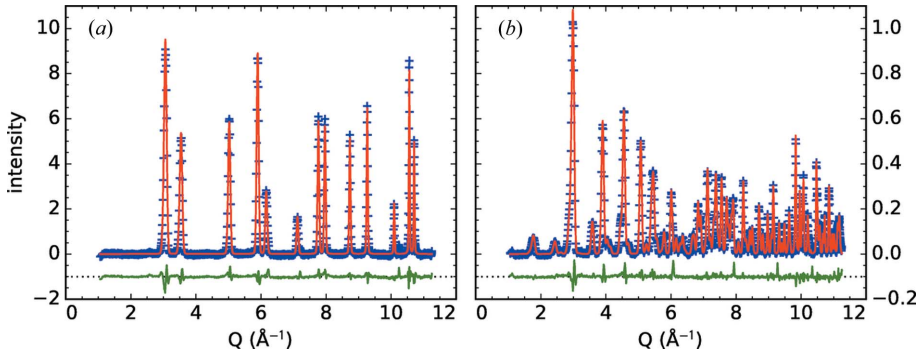

Figure 1
Rietveld refinements of neutron diffraction patterns from (*a*) nickel and (*b*) sapphire. The red line is the calculated and blue crosses the measured curves. Offset below, in green, is the difference curve. For both materials the instrumental and empty can background were removed prior to Rietveld refinement.

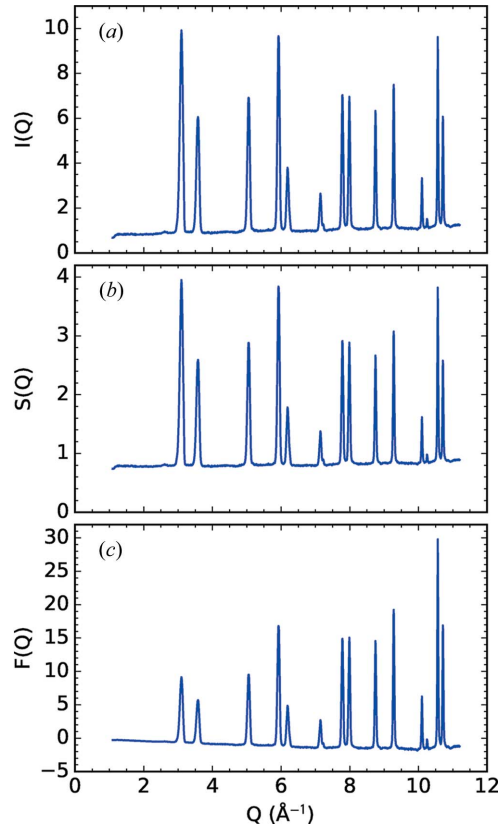

Figure 2
The intermediate results of PDF extraction from the nickel powder pattern measured at PEARL with monochromator setting 755. (*a*) The measured intensity $I(Q)$, (*b*) the structure function $S(Q)$ after scaling and polynomial corrections, and (*c*) the corresponding reduced structure function $F(Q)$.

reported by Wyckoff (1963) and Suh *et al.* (1988). The refinement of the sapphire standard was conducted with cell parameters fixed according to its NIST certificate and with refinable neutron wavelength, instrumental zero, atom positions and isotropic displacement parameters. The obtained results are in good agreement with literature values (Kirfel & Eichhorn, 1990; Lewis *et al.*, 1982; Ishizawa *et al.*, 1980; Newnham & de Haan, 1962; Lutterotti & Scardi, 1990).

3.2. PDF extraction

The background-corrected (*i.e.* instrumental and vanadium sample holder background removed) scattering profile for the nickel and sapphire samples was analyzed with *PDFgetN3*. The results of the various corrections contributing to the $F(Q)$ and $S(Q)$ functions for the nickel sample are presented in Fig. 2.

3.3. PDF analysis

The PDFs for nickel and sapphire were refined using the *SrFit* module in the *DiffPy-CMI* framework (see Fig. 3 and Fig. 5). This allowed for iterative refinement of a number of parameters, including process parameters (zero offset) and structural parameters (scale factor, Q-resolution damping factor, displacement parameters and unit-cell parameters), at the same time. The fitted zero correction compensated for minor imperfections in the monochromator crystal alignments and in sample centering. The PDF extraction does not yet include error propagation. The standard errors of the fitted variables were therefore evaluated by repeating PDF fits at Nyquist sampling ($\Delta r = \pi/Q_{max}$), which minimizes error correlations between data points and allows the estimation of PDF errors from the difference between measured and fitted curves (Farrow *et al.*, 2011; Bevington *et al.*, 1992). In order to extend the Q range we also recorded the scattering pattern for nickel using the 955 reflection of the monochromator, which translates to a constant wavelength of 0.955 Å. This increased the Q_{max} from 11.2 to 12.9 Å^{-1} and improved the r resolution in the PDF as displayed in Fig. 3(*b*). The refinement of the 955 data was conducted with a variable wavelength and with the cell parameter fixed to the outcome of the 755 fit. This refinement gave a neutron wavelength of 0.9554 (2) Å, which is in excellent agreement with an independent calibration from a Rietveld fit of the sapphire standard (λ = 0.95507 Å) and attests to the consistency and accuracy of the results at both monochromator settings. Table 2 presents a full summary

Table 2
Comparison of PDF analyses for nickel.

	PDFgetX3 Fig. 4	*PDFgetN3* (755) Fig. 3(*a*)	*PDFgetN3* (955) Fig. 3(*b*)
λ (Å)	0.14277	1.0989 (fixed)	0.95539 (16)
Q_{max} (Å^{-1})	26	11.2	12.9
Zero correction (°)	–	−0.391 (15)	−0.447 (17)
a	3.5238 (8)	3.5180 (6)	3.5180 (fixed)
Q_{damp} (Å^{-1})	0.056 (2)	0.037 (2)	0.041 (3)
δ_2	2.5 (2)	1.3 (6)	3.5 (7)
U_{iso} (Å^2)	0.005727 (92)	0.00437 (19)	0.00391 (20)
R_w	0.087	0.051	0.074

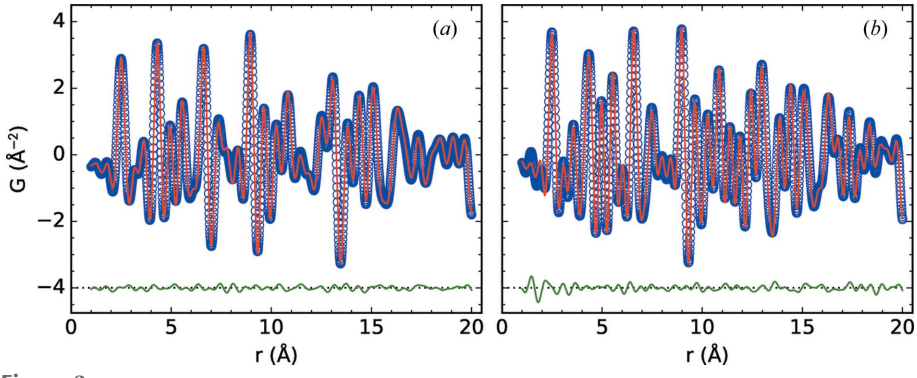

Figure 3
Refinement of nickel PDFs measured at the PEARL instrument using (*a*) monochromator reflection 755 (λ = 1.098 Å, Q_{max} = 11.2 Å^{-1}, R_w = 0.051) and (*b*) monochromator reflection 955. The second fit optimized the wavelength for a fixed unit cell obtained from the first fit and yielded (λ = 0.95539 (16) Å, Q_{max} = 12.9 Å^{-1}, R_w = 0.074). Experimental PDFs are plotted as blue circles and fitted curves as red lines, and the difference is offset below in green.

Table 3
Comparison of PDF analyses for sapphire.

	PDFgetX3 (NSLS-II) Fig. 5(*a*)	*PDFgetN3* (755) Fig. 5(*b*)
λ (Å)	0.2370	1.0989
Q_{max} (Å^{-1})	23.5	11.2
Zero correction (°)	–	−0.377 (15)
a (Å)	4.7572 (11)	4.7519 (12)
c (Å)	12.9855 (42)	12.9731 (28)
z (Al)	0.35236 (26)	0.35221 (37)
x (O)	0.30581 (93)	0.30664 (45)
Q_{damp}(Å^{-1})	0.01 (2)	0.031 (3)
δ_2	0.6 (5)	–
U_{iso} (Al) (Å^2)	0.00438 (36)	0.00157 (55)
U_{iso} (O) (Å^2)	0.00724 (68)	0.00361 (35)
R_w	0.164	0.071

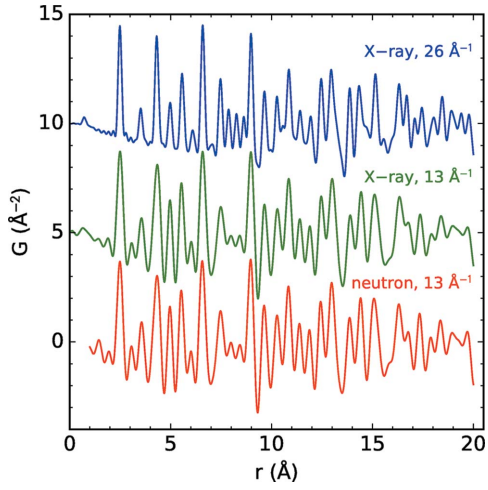

Figure 4
Comparison of Ni PDF obtained from constant-wavelength neutron scattering using the 955 monochromator setting (bottom red line) with the synchrotron X-ray PDF from Juhás *et al.* (2013) (top blue line), where the Q range extended to Q_{max} = 26 Å^{-1}. The middle green line is the X-ray PDF processed at the same Q_{max} = 12.9 Å^{-1} as the neutron scattering data. The PDF curves were extracted with *PDFgetN3* and *PDFgetX3*, respectively.

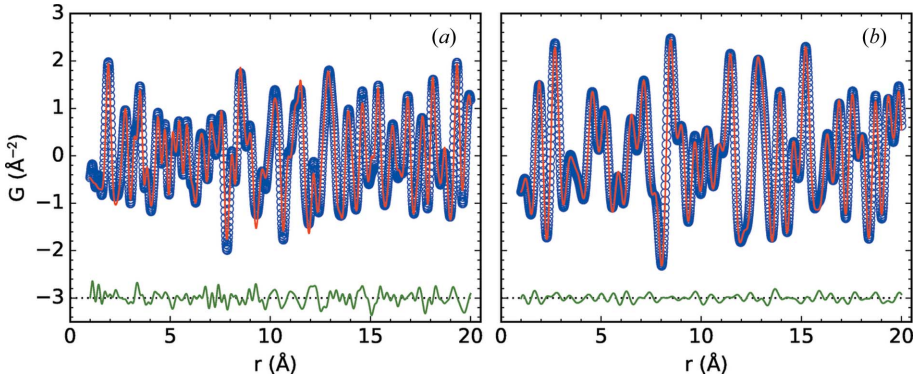

Figure 5
Refinement of sapphire PDFs measured by (*a*) NSLS-II synchrotron X-ray scattering at wavelength 0.2370 Å, Q_{max} = 23.5 Å^{-1}, and (*b*) CW neutron scattering using monochromator reflection 755, wavelength 1.098 Å, Q_{max} = 11.2 Å^{-1}.

of nickel fit results together with a fit to the synchrotron X-ray data from Juhás *et al.* (2013).

The unit-cell sizes found for nickel with neutron diffraction are slightly smaller (0.2%) than the values found above in the Rietveld refinement (Table 1), and are also smaller by a similar amount than that found in the PDF analysis of the synchrotron-derived data. Nevertheless, all values lie well within the range of 3.516–3.524 Å reported in the literature for nickel in cubic close-packed structure at ambient temperature (Wyckoff, 1963; Owen & Yates, 1936; Jette & Foote, 1935; Lundqvist, 1947; Suh *et al.*, 1988). The agreement between the X-ray and neutron PDFs is very good when they are processed with the same Q_{max}, as can be seen by comparing the bottom two curves in Fig. 4. The X-ray data processed with a higher Q_{max} are shown in the top curve for comparison. There is a significant loss of real-space resolution due to the limited Q range in the neutron measurement, which results in broader peaks in the neutron data. The shorter Q range also results in larger-amplitude termination ripples. This makes it hazardous to attribute meaning to individual peaks in the PDF, though it does not bias modeling which includes termination effects. As an example, a clear peak is evident at r = 3 Å, but there is no pair of atoms in the structure at that distance. These issues clearly improve when the data are collected at the 955 monochromator setting, and at either setting the data can be accurately modeled, as evidenced by the excellent match of the refined PDFs (Fig. 3). In general the peak amplitudes in X-ray and neutron PDFs differ because of the different scattering factors. However, this occurs only when peaks are formed by different atomic species, and for single-element materials such as nickel the PDF amplitudes from both techniques are equal.

The results from the model fits to the sapphire data are presented in Fig. 5 and Table 3. The refined values deviate only slightly from the parameters found by Rietveld analysis (Table 1) and from the X-ray PDF data. The unit-cell axes found in the PDF analysis are again 0.2% shorter than those found with Rietveld refinement, and slightly below the range found in the literature (4.754–4.7605 Å for *a*, and 12.9877–12.9956 Å for *c*) (Kirfel & Eichhorn, 1990; Lewis *et al.*, 1982; Ishizawa *et al.*, 1980; Newnham & de Haan, 1962; Lutterotti & Scardi, 1990). This deviation appears inconsequential for the overall structure as the refined fractional coordinates *z* (Al) and *x* (O) agree within their error estimates with the literature values (Newnham & de Haan, 1962). The X-ray PDF refinement of sapphire utilized data with Q_{max} about twice as large as the neutron case; however, it yielded a noticeably larger difference (Fig. 5) and a higher fit residual than the neutrons (R_w = 0.164 *versus* 0.071). The lower quality of the X-ray fit may be caused by valence deviations in the bonded Al—O sites, which affect their

actual scattering factors and the resulting PDF amplitudes. We find that the effect of valence on fits to these X-ray PDFs is not small. The reported $R_w = 0.164$ was obtained using scattering factors for neutral Al and O sites at valences 13 and 8. A trial refinement with ionic Al^{3+}, O^{2-} (valences 10, 10) actually gave a much worse fit ($R_w = 0.37$), revealing the high sensitivity of the PDF model to Al—O bonding and effective valences. It is beyond the scope of this paper to refine the valences to see whether this could improve the fit.

Finally, we note that we also used *PDFgetN3* to take intensity data from a time-of-flight neutron experiment that had been reduced to $I(Q)$ but not normalized or Fourier transformed, and it gave a comparable quality PDF to one calculated using all the corrections.

4. Conclusions

We have presented a new software program, *PDFgetN3*, for the extraction of pair distribution functions from powder neutron diffraction intensities. The comparison between results from Rietveld refinement and PDF analysis, as well as the comparison between neutron PDF analysis and X-ray PDF analysis, shows good agreement. The *ad hoc* correction method introduced in *PDFgetX3* is therefore also applicable in the PDF extraction with *PDFgetN3* presented here. The software is available for download at http://www.diffpy.org.

Acknowledgements

The authors thank Dr Milinda Abeykoon for essential help with synchrotron X-ray experiments.

Funding information

These measurements were conducted at the beamline 28-ID-2 of the National Synchrotron Light Source II, a US Department of Energy (DOE) Office of Science User Facility operated for the DOE Office of Science by Brookhaven National Laboratory under contract No. DE-SC0012704. PJ was supported by the New York State BNL Big Data Science Capital Project under the US Department of Energy contract No. DE-SC-00112704. SJLB was supported by the US Department of Energy, Office of Science, Office of Basic Energy Sciences (DOE-BES) under contract No. DE-SC00112704. JNL and ETCV acknowledge support by the Albemarle Catalysts Company BV. ETCV was also funded by the NWO (Netherlands Organization for Scientific Research) project TKINCI.2015.005.

References

Bevington, P. R., Robinson, D. K. & Bunce, G. (1992). *Data Reduction and Error Analysis for the Physical Sciences*, 2nd ed. New York: McGraw-Hill.
Billinge, S. J. L. (2010). *Physics*, **3**, 25.
Billinge, S. J. L. & Farrow, C. L. (2013). *J. Phys. Condens. Matter*, **25**, 454202.
Caglioti, G., Paoletti, A. & Ricci, F. P. (1958). *Nucl. Instrum.* **3**, 223–228.
Egami, T. & Billinge, S. J. L. (2012). *Underneath the Bragg Peaks: Structural Analysis of Complex Materials*, 2nd ed. Amsterdam: Elsevier.
Eijck, L. van, Cussen, L. D., Sykora, G. J., Schooneveld, E. M., Rhodes, N. J., van Well, A. A. & Pappas, C. (2016). *J. Appl. Cryst.* **49**, 1398–1401.
Farrow, C. L., Shaw, M., Kim, H.-J., Juhás, P. & Billinge, S. J. L. (2011). *Phys. Rev. B*, **84**, 134105.
Fischer, H. (2016). *SofqSoft: Software For Treating S(q) Neutron Scattering Data from Disordered Systems*, https://forge.epn-campus.eu/projects/sofqsoft.
Hammersley, A. P. (2016). *J. Appl. Cryst.* **49**, 646–652.
Hammersley, A. P., Svensson, S. O., Hanfland, M., Fitch, A. N. & Hausermann, D. (1996). *High. Pressure Res.* **14**, 235–248.
Howe, M. A. & McGreevy, R. L. Z. P. (1996). *CORRECT: A Correction Program for Neutron Diffraction Data.* Technical Report, The Studsvik Neutron Research Laboratory, Uppsala University, Sweden.
Ishizawa, N., Miyata, T., Minato, I., Marumo, F. & Iwai, S. (1980). *Acta Cryst.* B**36**, 228–230.
Jette, E. & Foote, F. (1935). *J. Chem. Phys.* **3**, 605–616.
Juhás, P., Davis, T., Farrow, C. L. & Billinge, S. J. L. (2013). *J. Appl. Cryst.* **46**, 560–566.
Juhás, P., Farrow, C., Yang, X., Knox, K. & Billinge, S. (2015). *Acta Cryst.* A**71**, 562–568.
Kirfel, A. & Eichhorn, K. (1990). *Acta Cryst.* A**46**, 271–284.
Lewis, J., Schwarzenbach, D. & Flack, H. D. (1982). *Acta Cryst.* A**38**, 733–739.
Lundqvist, D. (1947). *Ark. Mineral. Och Geol.* **24**, 1–12.
Lutterotti, L. & Scardi, P. (1990). *J. Appl. Cryst.* **23**, 246–252.
Newnham, R. E. & de Haan, Y. M. (1962). *Z. Kristallogr.* **117**, 235–237.
Owen, E. & Yates, E. (1936). *London Edinb. Dubl. Philos. Mag. J. Sci.* **21**, 809–819.
Peterson, P. F., Gutmann, M., Proffen, Th. & Billinge, S. J. L. (2000). *J. Appl. Cryst.* **33**, 1192.
Petkov, V. (1989). *J. Appl. Cryst.* **22**, 387–389.
Qiu, X., Thompson, J. W. & Billinge, S. J. L. (2004). *J. Appl. Cryst.* **37**, 678.
Soper, A. K. & Barney, E. R. (2011). *J. Appl. Cryst.* **44**, 714–726.
Suh, I.-K., Ohta, H. & Waseda, Y. (1988). *J. Mater. Sci.* **23**, 757–760.
Toby, B. H. & Von Dreele, R. B. (2013). *J. Appl. Cryst.* **46**, 544–549.
Wyckoff, R. W. G. (1963). *Crystal Structures*, Vol. 1, 2nd ed. New York: Wiley.